

FEM-based framework for the simulation of acoustic noise barriers

Jonathan Nowak¹, Andreas Fuchs¹

¹AIT Austrian Institute of Technology GmbH, 1210 Wien, Email: [jonathan.nowak, andreas.fuchs]@ait.ac.at

Introduction

Noise reducing devices (NRDs) such as noise barriers are a critical component in mitigating transportation-related noise pollution. In Europe, the EN 1793-5 standard provides a method for measuring and evaluating the in-situ sound reflection properties of noise barriers under direct sound field conditions. Noise barriers must often comply to specified minimum values for sound absorption, ensuring they effectively protect nearby residents from harmful noise levels. Therefore, ensuring that a noise barrier's design meets the desired sound reflection performance is crucial during product development. However, since a measurement according to EN 1793-5 requires manufacturing an element of at least $4\text{ m} \times 4\text{ m}$, measuring the performance of prototypes in real-world conditions can be resource-intensive, expensive, and challenging.

To address these challenges, Finite Element (FE) simulations offer a promising alternative to traditional measurement techniques. FE models can replicate the acoustical behavior of noise barriers in the setup defined in EN 1793-5, providing insights into their effectiveness without the need for manufacturing and real-world measurements.

This paper presents a Finite Element Method (FEM)-based framework simulating the acoustic properties of a representative fraction of the noise barrier. The NRDs' acoustically absorbing materials are characterized via impedance tube measurements with which their material parameters are fitted using a suitable material model. Subsequently, we model acoustic absorbers as equivalent fluids. By solving the Helmholtz equation via FEM, the sound pressure is computed at the microphone positions defined in EN 1793-5.

In this contribution, a validation of the framework against sound reflection measurements according to EN 1793-5 will be presented, using a common porous acoustic absorber mounted to a sound hard surface serving as an NRD.

EN 1793-5

This standard, defined in [1], specifies a robust in-situ measurement under direct sound field conditions for determining the sound reflection properties of noise barriers used to mitigate noise from road traffic. Using a loudspeaker and a microphone grid consisting of 9 microphones arranged in a regular grid, impulse responses are calculated. By comparing the reflected component and the incident reference component of these impulse responses, the reflection index $RI(f_j)$ may be computed in each third-octave band with the center-frequency f_j within $200 \leq f_j/\text{Hz} \leq 5500$. Time-domain windowing is used to filter parasitic reflections, e. g. ground reflections.

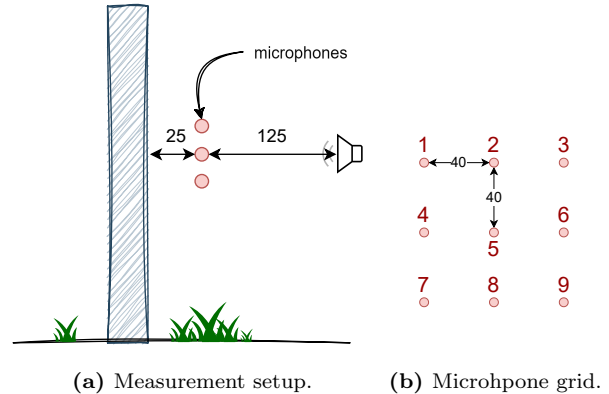


Figure 1: Positions of microphone grid and loudspeaker defined in EN 1793-5 with respect to the device under test (depicted in blue), dimensions in cm.

The measurement setup is depicted in Fig. 1a and a front view of the 9 microphone positions and the corresponding numbering can be seen in Fig. 1b. The spacing between the microphones is 0.4 m. The microphone grid is placed in a distance of 0.25 m to the reference plane in front of the NRD, where the reference plane is a vertical surface that contains the noise barrier's most protruding point. The loudspeaker's center is placed in front of the microphone number 5 at a distance of 1.25 m.

The reflection index is calculated in each of the n_j third-octave bands with center frequencies f_j and widths Δf_j according to

$$RI_j = \frac{1}{n_k} \sum_{k=1}^{n_k} \left[\frac{\int_{\Delta f_j} |\mathcal{F}[h_{r,k}(t) w_{r,k}(t)]|^2 df}{\int_{\Delta f_j} |\mathcal{F}[h_{i,k}(t) w_{i,k}(t)]|^2 df} C_{\text{geo},k} C_{\text{dir},k}(\Delta f_j) C_{\text{gain},k}(\Delta f_g) \right]. \quad (1)$$

Here, n_k denotes the number of microphones considered, \mathcal{F} is the symbol of the Fourier transform, $h_{r,k}$ denotes the reflected component of the impulse response taken in front of the sample under test at the k -th microphone position and $w_{r,k}(t)$ is the corresponding Adrienne temporal window defined in [1]. Variables with an index "i" instead of "r" denote the corresponding quantities of the incident reference component of the free-field impulse response, obtained via a separate free-field measurement. Further, the correction factors $C_{\text{geo},k}$, $C_{\text{dir},k}(\Delta f_j)$ and $C_{\text{gain},k}(\Delta f_g)$ are applied for geometrical divergence at the k -th microphone position, for the directivity of the used loudspeaker and for a potential change in the amplification settings of the loudspeaker, respectively. While $C_{\text{geo},k}$ is not a function of frequency, the other two correction factors depend on frequency.

The factor $C_{\text{geo},k}$ is calculated via

$$C_{\text{geo},k} = \left(\frac{d_{r,k}}{d_{i,k}} \right)^2, \quad (2)$$

where $d_{i,k}$ is the distance from the loudspeaker's front panel to the k -th microphone point and $d_{r,k}$ is the length of the path from the loudspeaker to the reference plane and back to the k -th microphone point following specular reflection. This factor accounts for the decrease in amplitude between source and receiver position: The loudspeaker is assumed as an acoustic monopole and the noise barrier is assumed as a sound-hard plane. The factor $C_{\text{geo},k}$ is the squared ratio between the amplitude decrease for the direct path $d_{i,k}$ between source point and microphone k , compared to the decrease in amplitude for the reflected path $d_{r,k}$. Eq. (2) may be derived from the well-known free-field Green's function g for acoustic monopoles

$$g(d, \omega) = \frac{1}{4\pi d} e^{jk d}, \quad k = \frac{\omega}{c} = \frac{2\pi f}{c}, \quad (3)$$

with the wave number k , the angular frequency ω , the speed of sound c , and the distance between source and receiver position d .

For details on the measurement procedure, computation of the impulse responses and reflected component, and calculation of the correction factors see [1].

FE simulations

For the numerical computation of the reflection index $RI_j(f)$ according to EN 1793-5, a 2D fraction of the noise barrier and the surrounding air is modeled with FEM. This amounts to solving the Helmholtz equation, the wave equation in frequency domain, with respect to given boundary conditions, see Eq. (4), with the media's compression modulus K and density ρ and a generalized source distribution \mathcal{F} . The modeled section contains the microphone positions 2, 5 and 8, see Fig. 1b. Therefore, the evaluation of Eq. (1) is only performed for $k = [2, 5, 8]$. The simulations were carried out with the open-source software openCFS [2].

$$\nabla \cdot \rho \nabla p_a + \omega^2 \frac{1}{K} p_a = \mathcal{F}. \quad (4)$$

Here, the loudspeaker is modeled as a point source and the free-field radiation condition at the boundaries is accomplished with a Perfectly Matched Layer (PML), see e.g. [3]. As surrogate noise barrier serve multiple panels of Basotect[®], a porous acoustic absorber based on melamine resin, with different thicknesses which are mounted to a sound-hard surface. The absorbing property of the noise barrier's material, in the considered case a porous acoustic absorber, is modeled with an equivalent fluid approach. Here, the material's compression modulus K and density ρ in Eq. (4) become complex-valued in order to model sound attenuation within the absorber, see e.g. [4, 5]. By modeling this region as equivalent fluid, the absorber's shape and sound incidence at oblique angles may be fully considered.

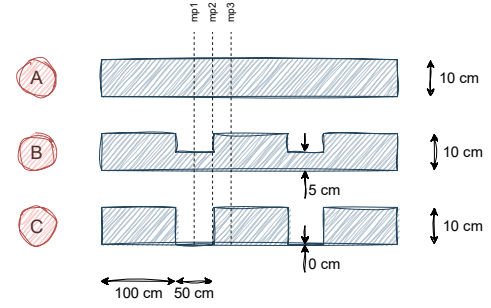


Figure 2: Sketch of the considered surrogate noise barrier configurations consisting of a porous acoustic absorber with different thicknesses. Indicated measurement points (mp) are only relevant for configurations B and C.

Three configurations – named A, B and C –, will be investigated. The absorber panels have thicknesses of 10 cm and 5 cm and are arranged according to the sketches shown in Fig. 2. In configuration C, a combination of 10 cm Basotect and a sound-hard surface is considered.

Since the excitation is provided by a monopole, in the simulation, the correction factor for the directivity amounts to $C_{\text{dir},\text{sim},k} = 1$ and, as no real measurement equipment is used, also the relation $C_{\text{gain},\text{sim},k} = 1$ holds. In contrast, the correction for geometrical divergence has to be considered in the simulation. However, since the simulations are carried out in 2D, Eq. (2) may not be used. The two-dimensional free-field Green's function is defined as [6]

$$g_{2D}(d, \omega) = \frac{j}{4} H_0^{(2)}(kd), \quad (5)$$

where $H_0^{(2)}$ is the Hankel function of order 0 and 2nd kind. Therefore, the adapted correction factor in the two-dimensional simulation case becomes frequency-dependent and reads as

$$C_{\text{geo},2D,k} = \left(\frac{H_0^{(2)}(k d_{i,k})}{H_0^{(2)}(k d_{r,k})} \right)^2. \quad (6)$$

Modeling of noise barrier

As mentioned, sound propagation within the absorber region (depicted in blue in Fig. 1a) is modeled by an equivalent fluid. There, the complex values for K and ρ are computed with the Johnson-Champoux-Allard-Lafarge (JCAL) model [7], a semi-empirical material model. Its parameters ζ_i , including the materials porosity and flow resistivity, are fitted via impedance tube measurements, according to ISO 10534-2:2023 [8]. These measurements of the material's reflection factor r require cylindrical samples of the absorber. The fitting is performed using a Genetic Optimization. Its cost function J reads as

$$J(\omega) = \|r_{\text{meas}}(\omega) - r_{\text{calc}}(\omega, \zeta_i)\|^2, \quad (7)$$

with the measured reflection factor r_{meas} and the calculated reflection factor r_{calc} which depends on the JCAL model parameters to be determined.

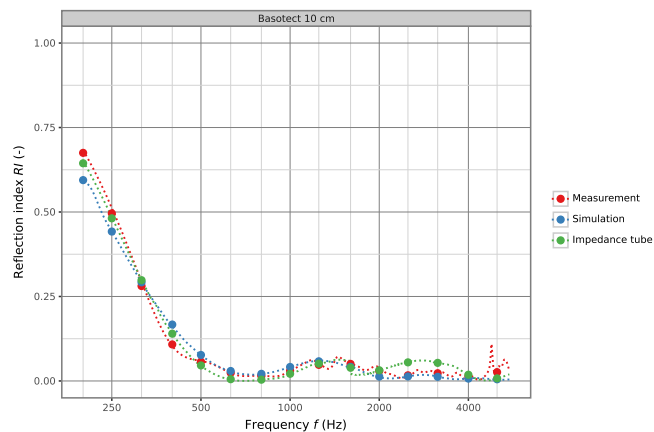


Figure 3: Comparison of RI -values obtained via EN 1793-5 with measured (red) and simulated (blue) data and impedance tube measurements (green).

Comparison of RI : measured and simulated

First, only configuration A (Fig. 2) is considered. Here, since the absorber panels, i. e. the surrogate noise barrier, have a uniform thickness of 10 cm, there are three options to measure or simulate RI , namely the measurement with an impedance tube, and the evaluation according to EN 1793-5 with either measured or simulated sound pressure data. Again, one has to bear in mind that for the latter method, only the center column of microphones, i. e. microphones 2, 5 and 8 (Fig. 1b) are considered in both the simulation and the measurement evaluations. A comparison in Fig. 3 shows very good agreement between these three evaluation methods. The narrow-band spectra are depicted as dashed lines and the corresponding third-octave band data are shown as filled circles.

When measuring non-flat or non-homogeneous noise barriers according to EN 1793-5, it might be necessary to consider more than one measurement point. Here, the designation ‘measurement point’ is to be understood as the position of the loudspeaker and the middle microphone (mic. 5) relative to the noise barrier. Therefore, for configurations B and C three measurement points, indicated as “mp1”–“mp3” in Fig. 2, were considered. Measurement point mp1 is located in the middle of the most recessed part of the surrogate noise barrier, mp2 is located at the edge between most recessed and most protruding part and mp3 is positioned in front of the 10 cm-panel at a distance of 25 cm from mp2. It has to be mentioned that not all of those measurement points are required according to the standard. However, we aim at comparing measurements and FE simulations and not at carrying out a strict standard measurement.

In doing so, we compare the values of RI obtained via EN 1793-5 with either measured or simulated sound pressure data for configurations B and C for three measurement points each. The results may be taken from Fig. 4. While the three measurement points are depicted in the rows of the graph, configuration B is shown in the left col-

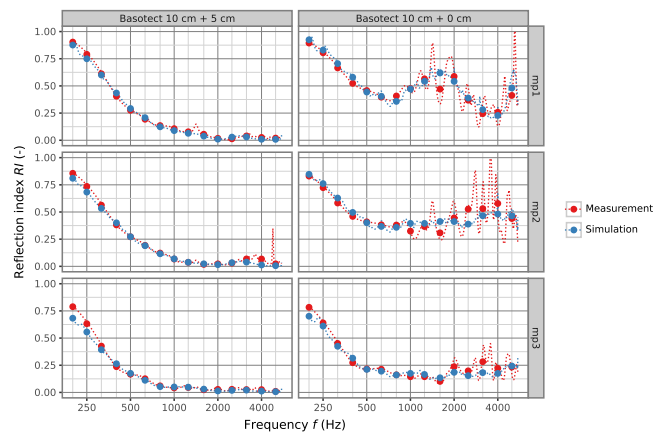


Figure 4: Comparison of reflections indices obtained via measurements and simulation for configurations B and C at different measurement points.

umn and configuration C is shown in the right column. Again, there is good agreement between simulations and measurements especially for configuration B. At frequencies $f > 1000$ Hz the measurements of configuration C start to oscillate and therefore the deviation between measurement and simulation for some of the third-octave band values, e. g. at $f_j = 1600$ Hz for mp1 and mp2 are higher. Oscillations of RI at higher frequencies for noise barriers with (nearly) sound hard elements are a known characteristic of the measurement method defined by the standard. Why these oscillations are not so pronounced in the simulation can only be speculated at this point in time. Possible reasons may be inaccuracies in the positioning of the measurement microphones, longer impulse responses of an actual loudspeaker which are windowed by the Adrienne temporal window or reflections at the microphones or the mounting equipment itself.

However, the course of all of the measurement curves can be predicted very well by the simulations.

Comparison of single-number rating DL_{RI}

In a last step, the single-number rating DL_{RI} defined in EN 1793-5 [1] is considered. This value is mainly used to assess a noise barrier and to compare different NRDs with each other. It calculates as a weighted sum of the reflection index $RI(f_j)$, where the weights are defined according to the normalized traffic noise spectrum L_j defined in [9]. With this weighting, for noise barriers installed along roads, the frequency bands around 1 kHz are most strongly weighted. The definition of the single-number rating DL_{RI} reads as

$$DL_{RI} = -10 \log \left[\frac{\sum_j RI_j 10^{0.1L_j}}{\sum_j 10^{0.1L_j}} \right]. \quad (8)$$

A correlation plot between the calculated and simulated DL_{RI} -values for configurations A–C and all measurement points shows again very good agreement between simulations and measurements, see Fig. 5. Further, the graph shows that configuration A (“Baso. 10cm”, red) has the highest DL_{RI} -value, followed by configurations B

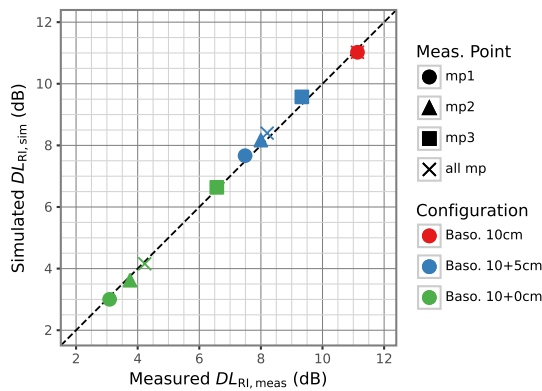


Figure 5: Measured and simulated single-value ratings DL_{RI} of all considered configurations and measurement points.

(“Baso. 10cm+5cm”, blue) and C (“Baso. 10cm+0cm”, green), which is as expected since the volume of sound absorbing material decreases for increasing configuration labels. Additionally, one can see that mp3 (square marker) has the highest DL_{RI} -value within configurations B and C, since this measurement point is always in front of the absorber panel with 10 cm thickness. The single-number rating calculated from the arithmetically averaged RIs of all measurement points for each configuration is marked with an ‘x’ (“all mp”).

In addition, since the FEM calculates the acoustic pressure in each node of the computational mesh and not only at the microphone positions of the standard, a visualization of the sound field in front of the noise barrier may be obtained which may provide additional valuable insight for e. g. product development. Unfortunately, due to lack of space these visualizations cannot be shown here.

Summary and outlook

This contribution presented a framework for the prediction of the reflection index of noise barriers according to the international standard EN 1793-5. The framework is based on the Finite Element (FE) Method and the geometric structure of noise barriers can be taken into account. Their acoustically absorbing properties are incorporated via the equivalent fluid approach where the complex-valued material parameters are fitted from impedance tube measurements using an appropriate material model.

The framework is validated with 2D FE simulations and measurements of a porous acoustic absorber mounted to a sound-hard surface in three different configurations. Results showed good agreement of simulated and measured sound reflection index within the considered frequency range of the third-octave bands with center frequencies between 200 Hz and 5500 Hz. Also, the derived single-number rating DL_{RI} showed a strong correlation between simulations and measurements.

An extension of the framework to 3D is possible. This would open up the possibility for the simulation of the remaining microphone positions in the side columns and more complex barrier geometries. However, due to the

increased degrees of freedom in the 3D case, the memory requirements and simulation times will increase significantly.

Since the validation of the two-dimensional simulations against real-life measurements provides promising results, using the framework for the optimization of noise barriers regarding its material and geometry can be considered. If many different variations shall be investigated, 2D simulations are preferred due to the aforementioned lower required computational power. Moreover, the simulations may provide valuable input for the further development of the standard, for example regarding the necessity of additional measurement points for non-flat and/or non-homogeneous noise barriers or its exact positions.

References

- [1] EN 1793-5:2016, Road traffic noise reducing devices – Test method for determining the acoustic performance – Part 5: Intrinsic characteristics – In situ values of sound reflection under direct sound field conditions, 2016.
- [2] Verein zur Förderung der Software openCFS [Association for the Promotion of the Software openCFS]. openCFS. 2021. URL: <https://opencfs.org/> (visited on 03/26/2025).
- [3] M. Kaltenbacher. Numerical Simulation of Mechatronic Sensors and Actuators: Finite Elements for Computational Multiphysics. 3rd ed. Springer, 2015.
- [4] Jean Allard and Nouredine Atalla. Propagation of Sound in Porous Media: Modelling Sound Absorbing Materials. 2nd ed. Wiley, 2009. ISBN: 0470746610.
- [5] François-Xavier Bécot, Luc Jaouen: An alternative Biot’s formulation for dissipative porous media with skeleton deformation. J. Acoust. Soc. Am. 1 December 2013; 134 (6): 4801-4807. <https://doi.org/10.1121/1.4826175>
- [6] A. Hirschberg and S.W. Rienstra. An Introduction to Acoustics. IWDE-Report. 2021. URL: <https://www.win.tue.nl/~sjoerdr/papers/boek.pdf> (visited on 03/26/2025).
- [7] Denis Lafarge: Dynamic Compressibility of Air in Porous Structures at Audible Frequencies. In: The Journal of the Acoustical Society of America 102 (4 Oct. 1997). DOI: 10.1121/1.41
- [8] ISO 10534-2:2023, Acoustics – Determination of acoustic properties in impedance tubes – Part 2: Two-microphone technique for normal sound absorption coefficient and normal surface impedance
- [9] EN 1793-3:2016, Road traffic noise reducing devices – Test method for determining the acoustic performance – Part 3: Normalized traffic noise spectrum, 1997.